

## MULTI-SCALE ANALYSIS ON 3D FLOW STRUCTURES BEHIND A WALL-MOUNTED SHORT CYLINDER CONTROLLED BY USING A FRONT INCLINED HOLE

Hiroka Rinoshika  
Department of Mechanical Systems Engineering  
Yamagata University  
4-3-16 Jonan, Yonezawa-shi, Yamagata, Japan

Akira Rinoshika  
Department of Mechanical Systems Engineering  
Yamagata University  
4-3-16 Jonan, Yonezawa-shi, Yamagata, Japan

Masato Akamatsu  
Department of Mechanical Systems Engineering  
Yamagata University  
4-3-16 Jonan, Yonezawa-shi, Yamagata, Japan

### ABSTRACT

This paper deals with the three-dimensional (3D) wake structures of a wall-mounted short circular cylinder, which are controlled by the flow issuing from a front inclined hole (FIH) drilled from the front side surface to the free end surface in the short cylinder. The 3D velocity fields are instantaneously measured at a Reynolds number of 10720 based on high-resolution tomographic particle image velocimetry (Tomo-PIV) in a water tunnel. A 3D W-type arch vortex is observed behind the short FIH cylinder. Compared with the standard cylinder, the 3D W-type arch vortex exhibits a large peak or convex at center of the horizontal part and collapses more rapidly at the downstream for the FIH cylinders. The flow from the FIH may increase the rear recirculation region, and its height may effectively control the vortical structures. A 3D wavelet multiresolution analysis is employed to decompose the instantaneous 3D velocity fields measured by the Tomo-PIV. The large-scale streamwise vortices in the FIH cylinder wakes are smaller than those in the standard cylinder wake, and this becomes more evident as the hole height increases. However, 3D time-averaged large-scale arch vortical structures becomes stronger.

### INTRODUCTION

Wall-mounted finite-length circular cylinders originate a strongly three-dimensional (3D) complex wake flow, which differs from that of an infinite circular cylinder (Rinoshika and Zhou, 2005). Due to the existence of the free end of the cylinder and the connection between the cylinder and the wall, such 3D flow structures are greatly influenced by the aspect ratio (the ratio of height to diameter) of the cylinder. The details on finite-height cylinders were described by Sumner (2013). Zhu et al. (2017) first measured the 3D flow structures behind a wall-mounted cylinder with an aspect ratio of 2 by tomographic PIV (Tomo-PIV), and found an instantaneous and mean 3D M-shape arch vortex. Recently, the 3D multiscale wake structures of a wall-mounted circular cylinder having an aspect ratio of 1 were investigated by Rinoshika et al. (2020) based on Tomo-PIV and a 3D wavelet transform; they found a strong 3D W-type arch vortex behind the short cylinder, and this was also observed in the time-averaged intermediate-scale structures.

Even though many investigations have revealed the flow structures behind short cylinders, few studies have focused on controlling the vortex-induced drag of a wall-mounted short cylinder. This would have wide-ranging engineering

applications in drag control for the design of offshore structures and increasing the efficiency of thermofluid systems, such as buildings, heat sink compounds, and the control surfaces on automobiles, aircraft, and underwater vehicles. Recently, the drilling of a front inclined hole (FIH) passing from the front side to the free end surface induces the increases of the rear separation region and Reynolds shear stress, and results in the increase of drag although it reduces the separation region on the free end surface (Rinoshika and Rinoshika, 2019). Such FIH short cylinders may be applied to control the offshore (breakwater) structures for reducing wave and Tsunami energies. However, how the flow that issues from the FIH affects the 3D wake structures of wall-mounted short cylinders remains unclear. This is the motivation for the present investigation.

In this paper, to clarify how the flow issuing from an FIH drilled from the front side to the free end of a wall-mounted short cylinder affects the 3D flow structures behind the cylinder, the instantaneous 3D velocity fields around the FIH and standard cylinders are first measured by Tomo-PIV. Then 3D orthogonal wavelet multiresolution analysis is used to decompose the instantaneous 3D velocity fields of the Tomo-PIV data, allowing their various scale 3D flow structures to be analysed.

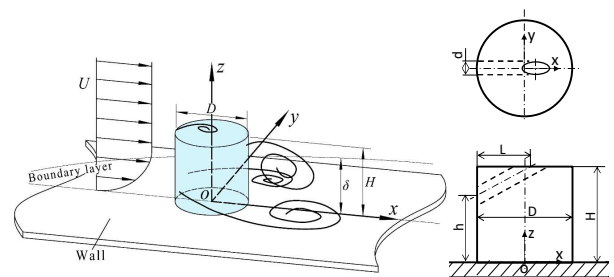


Figure 1 Model of wall-mounted short circular cylinder.

### EXPERIMENTAL SETUP AND METHODS

A short circular cylinder of diameter  $D = 70$  mm and height  $H = 70$  mm (aspect ratio  $H/D = 1$ ), as shown in Fig. 1, was placed on the bottom wall of a circular open water tunnel. This experiment was performed at a free stream velocity of  $U = 0.162$  m/s, corresponding to a Reynolds number  $Re = 10720$ . To control the complex 3D wake structures, an inclined hole of diameter  $d = 10$  mm ( $d/D = 0.14$ ), as shown on the right side of Fig. 1, was drilled from the front side to the free end of a wall-mounted short cylinder, which generates a flow issuing from the

free end. To evaluate the effect of the FIH position on the wake structures, three kinds of FIH cylinders were constructed with different heights of  $h = 20$  mm, 35 mm, and 50 mm (corresponding to  $h/D = 0.29$ , 0.5, and 0.71) from the flat plate on the front side of cylinder; these are referred to as FIH20, FIH35, and FIH50, respectively.

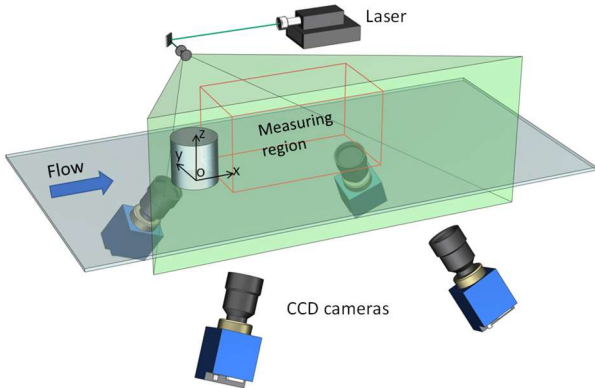


Figure 2 Tomo-PIV setup.

Figure 2 shows the experimental apparatus of the Tomo-PIV measurements. A dual-head Nd:YAG laser (500 mJ/pulse) having a 120-mm-thick light sheet was used. Four high-resolution (6600×4400 pixels) double-exposure charge-coupled device cameras recorded the measurement domain simultaneously. A synchronizer controlled the laser and cameras and produced a sampling frequency of 0.25 Hz. In this study, the measurement volume covered the domain of  $235 \times 140 \times 100$  mm<sup>3</sup> behind the cylinder. By using a multipass correlation analysis with a deforming interrogation window, the 3D vector field was calculated. The interrogation volume was  $32 \times 32 \times 32$  voxels with 50% overlap in the final pass, resulting in a 3D velocity vector field of  $101 \times 57 \times 40$  and giving a spatial resolution of 2.4 mm and a vector pitch of 2.4 mm.

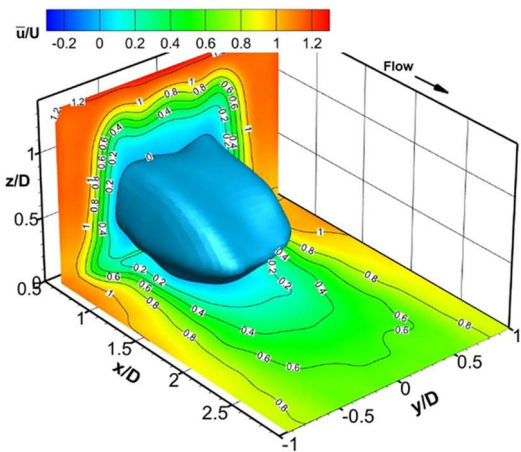
## RESULTS AND DISCUSSION

### Time-averaged 3D flow structures

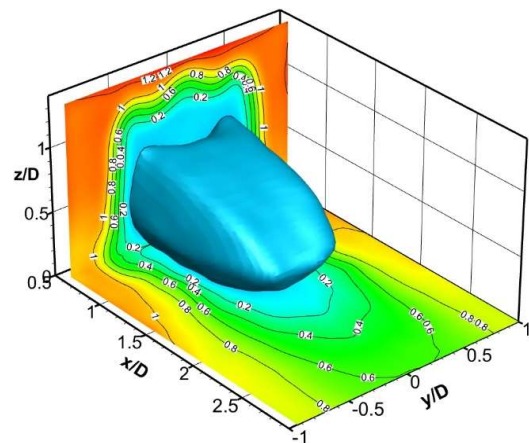
The 3D isosurfaces of  $\bar{u}/U = 0$  behind the FIH cylinders and the standard cylinder are shown in Figure 3. Here two contours of the streamwise velocity in the  $(x, y)$  of  $z/D = 0.04$  and  $(y, z)$  of at  $x/D = 0.7$  are also plotted in Figure 3. The isosurface of  $\bar{u}/U = 0$ , averaged over 400 Tomo-PIV snapshots, shows a 3D rear recirculation zone. A top concavity isosurface is clearly observed near the plane of  $y/D = 0$  in the standard cylinder [Figure 3(a)], generated by the downwash flow from the free end. The separation region gradually contracts along the main flow direction, and comes to an end downstream at around  $x/D = 1.6$  because of the interaction of the vortex generating from the side and free end of the cylinder. In the case of the FIH cylinders, as shown in Figures. 3(b)–3(d), a large top concavity isosurface appears near the plane of  $y/D = 0$  by the flow issuing from the FIH in the short cylinder. The separation region in the streamwise direction of FIH cylinders is larger than that of the standard cylinder because the issuing flow from the hole of free end increases the separation region. The isosurface heights of FIH cylinders are also slightly higher than that of the standard cylinder since the issuing flow from the FIH prevents downwash flow. As the height of front hole becomes higher, the height of separation region increases slightly. It is clear that the flow

issuing from the FIH of the cylinder increases the rear recirculation region and is related to increasing drag force. It may be used as an important application in the offshore structures and heat exchangers, especially suppressing Tsunami energy.

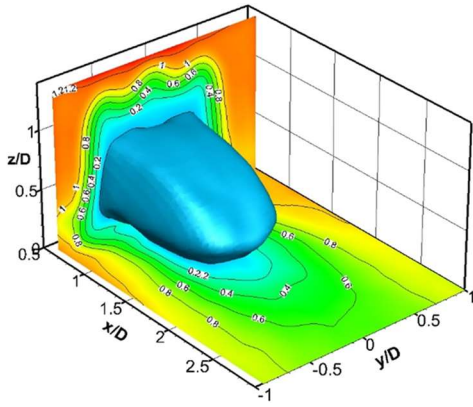
Figure 4 shows the comparison of the 3D time-averaged isosurfaces of  $Q/(U/D)^2 = 0.7$  colored by the streamwise vorticity  $\bar{\omega}_x D/U$  between the standard and FIH cylinders. The arch vortex shape of the standard cylinder wake, as shown in Figure 4(a), changes from a W shape to an M shape along the flow direction due to the strong downwash flow near the central plane. However, since the issuing flow from the hole of free end induces a large separation flow and unsteady flow (Rinoshika and Rinoshika 2019), the arch vortex shapes of the FIH cylinders collapses easily at the downstream. As the height of the FIH decreases, the destruction of the M-shape head becomes more evident, because the hole issuing flow from the free end forms a large angle with the main flow direction, and produces a separation flow on the free end. Moreover, the shape of arch structure gradually recovers to that of the standard cylinder as increasing the height of front hole (i.e., the angle decreases). These results indicate that the flow from the FIH cylinder may break down and control the large-scale vortical structures of the short cylinder wake. This result may be applied to the drag control.



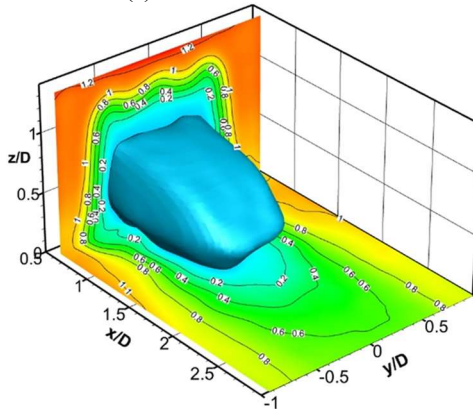
(a) Standard



(b) FIH20

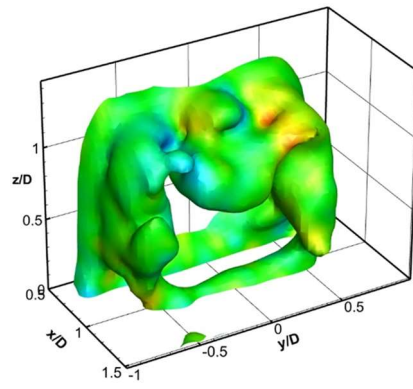


(c) FIH35

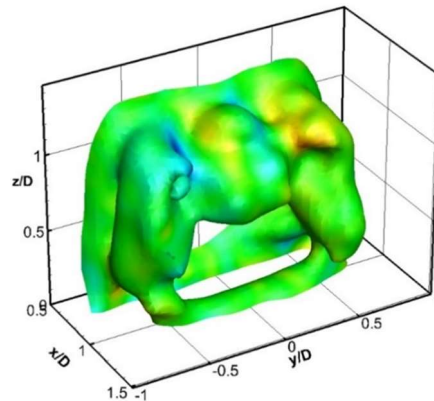


(d) FIH50

Figure 3 Mean isosurface of  $\bar{u}/U = 0$  with the contours of the streamwise velocity in the  $(x, y)$  of  $z/D = 0.04$  and  $(y, z)$  of  $x/D = 0.7$ .

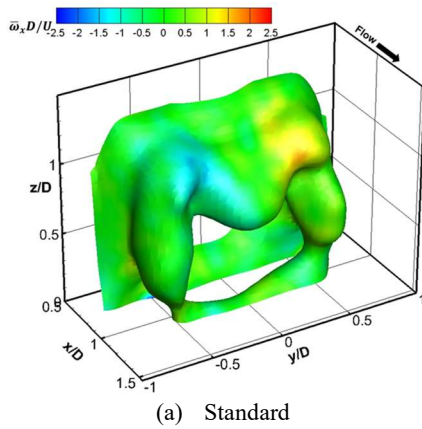


(c) FIH35

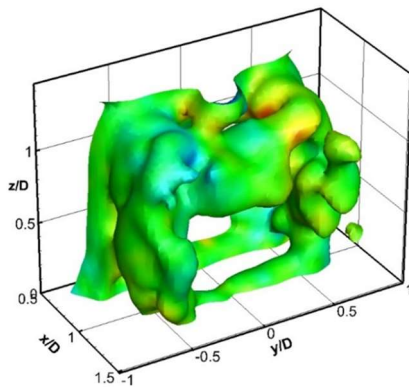


(d) FIH50

Figure 4 Mean isosurface of  $Q/(U/D)^2 = 0.7$  colored by the streamwise vorticity  $\bar{\omega}_x D/U$ .



(a) Standard



(b) FIH20

### Instantaneous 3D multiscala wake structures

Figure 5 shows the 3D distribution of the instantaneous  $Q$  criterion with the isosurface of  $Q/(U/D)^2 = 5.5$  colored by the streamwise vorticity  $\omega_x D/U$  around the standard and FIH cylinders. This figure shows the complexity of 3D instantaneous vortical structures of various scales. Large-scale streamwise vortices (Zhu et al. 2017) (indicated by 3 and 4) near the cylinder are clearly observed, and the W-type arch vortex rapidly breaks down into several fragments (indicated by 2) downstream.

Figure 6 shows the instantaneous 3D  $Q_1/(U/D)^2 = 1.0$  isosurface of large-scale structures, colored by the streamwise vorticity  $\omega_{x1} D/U$  in the standard and FIH cylinder wakes, based on the 3D wavelet multiresolution analysis. A large-scale arch vortex, corresponding to the vortical structure labelled 2 in Figure 5, is clearly observed in the standard and FIH cylinders. Meanwhile, large-scale streamwise vortices (labelled by 3 and 4) are also extracted, which match the instantaneous flow structures in Figure 5. They go through the center of the arch vortex and develop downstream, dominating the flow structures downstream. Compared to the large-scale arch structure (labelled 2) of standard cylinder, more large-scale arch structures (labelled 1 and 2) are observed in the FIH cylinders. As the height of the FIH decreases, the size of large-scale streamwise vortex decreases because the hole issuing flow from the free end forms a large angle with the main flow direction, which induces a strong upwash flow and limits to the generation of streamwise vortex near the cylinder. These results indicates that the flow issuing from the FIH dominates and controls the large-scale flow structures including the large-scale streamwise vortex.

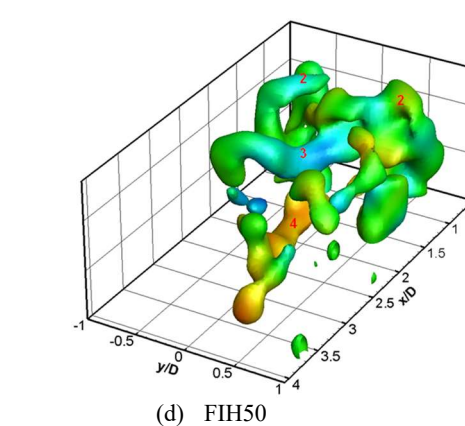
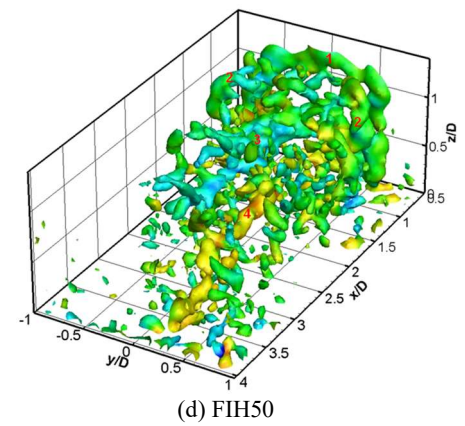
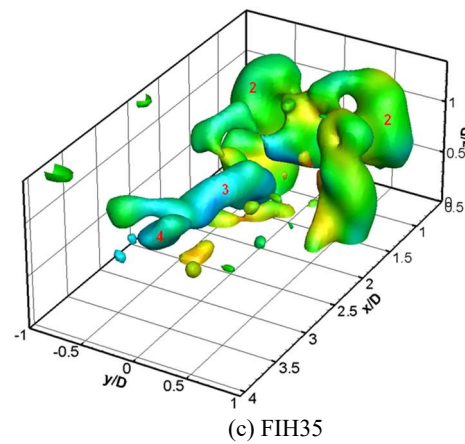
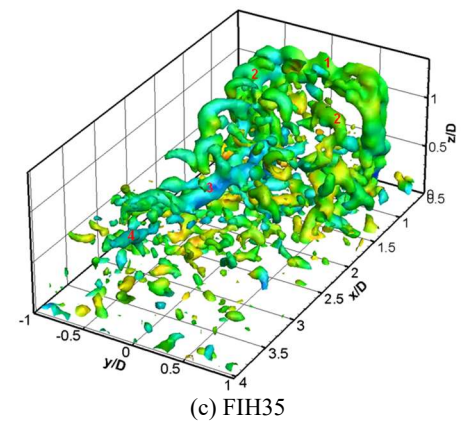
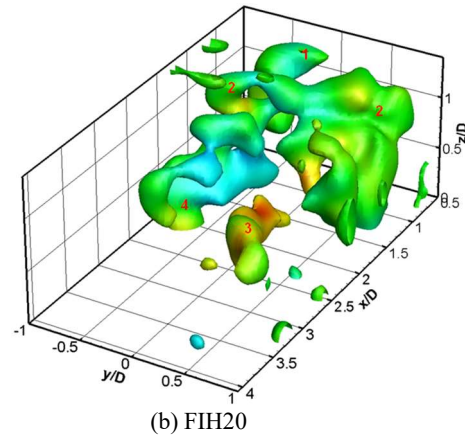
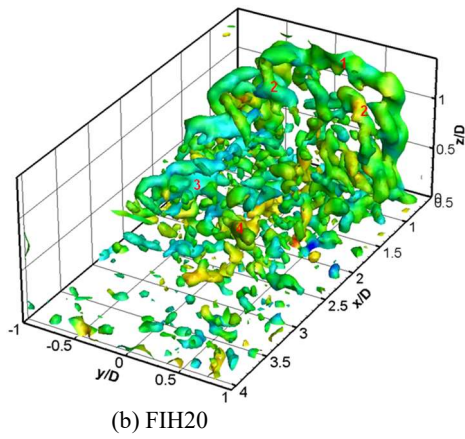
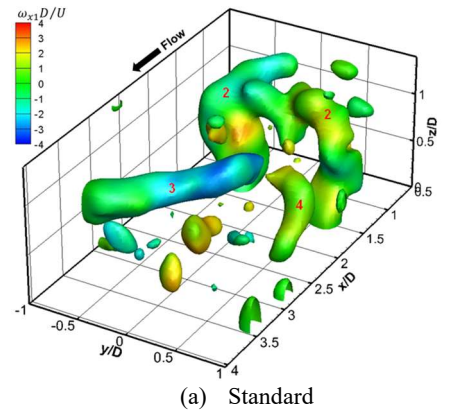
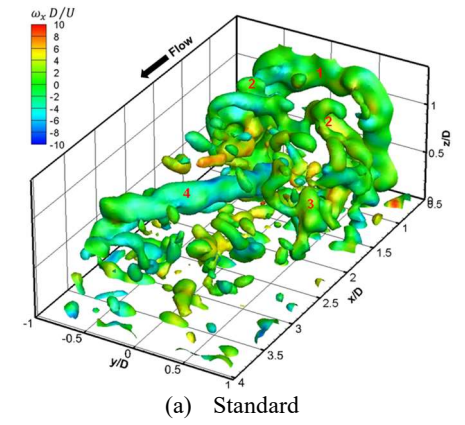
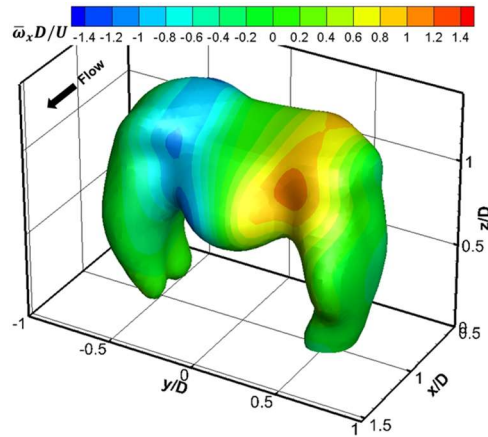


Figure 5 Instantaneous 3D isosurface of  $Q/(U/D)^2 = 5.5$  colored by the streamwise vorticity  $\omega_x D/U$  around various cylinders.

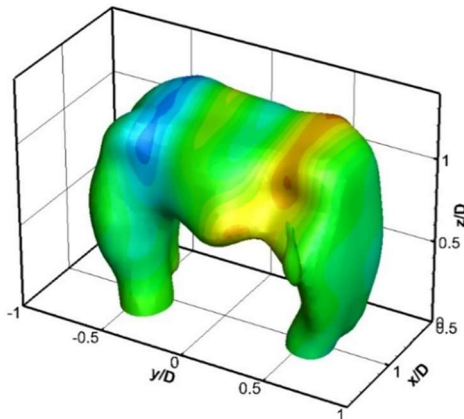
Figure 6 Instantaneous 3D large-scale isosurface of  $Q_1/(U/D)^2 = 1.0$  colored by the streamwise vorticity  $\omega_{x1} D/U$  around various cylinders.

### Time-averaged 3D multiscale wake structures

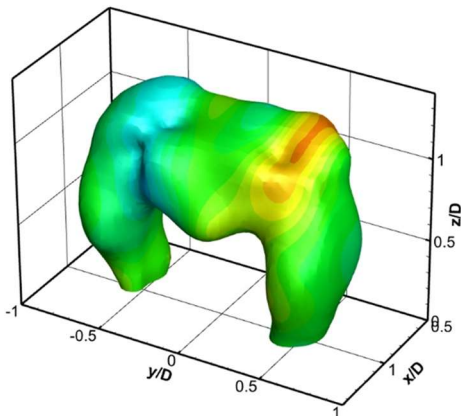
The time-averaged 3D large-scale isosurface  $Q_1/(U/D)^2 = 0.7$  of large-scale structure (level 1) based on the 3D wavelet multiresolution analysis, as shown in Figure 7, exhibits a large-scale 3D arch vortex behind the standard cylinder and FIH cylinders. A pair of tip vortices near two convex parts of the horizontal part of the arch vortex can be clearly seen based on the contour of time-averaged streamwise vorticity  $\bar{\omega}_{x1}D/U$ . The  $Q_1/(U/D)^2$  isosurfaces of the FIH cylinders are slightly larger than that of the standard cylinder, which implies stronger large-scale structures in the FIH cylinders.



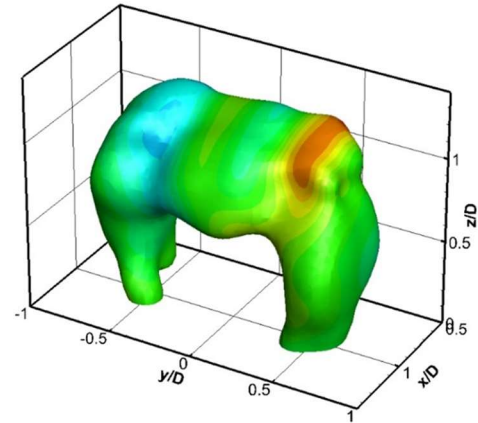
(a) Standard



(b) FIH20



(c) FIH35



(d) FIH50

Figure 7 Time-averaged 3D large-scale isosurface of  $Q_1/(U/D)^2 = 0.7$  colored by the streamwise vorticity  $\bar{\omega}_{x1}D/U$  around various cylinders.

### CONCLUSIONS

This paper has addressed the applications of Tomo-PIV measurements and 3D wavelet analysis to reveal the 3D multiscale flow structures behind wall-mounted FIH short cylinders. Compared with a wall-mounted standard short cylinder, the main results are as follows.

(1) A large rear recirculation region and a strong 3D W-type arch vortex appear behind FIH cylinders, which increases with decreasing the height of the FIH.

(2) An instantaneous W-type arch vortex and streamwise vortices are also observed in the near-wake region, and break down more quickly into several fragments downstream.

(3) Based on the 3D wavelet analysis, the size of large-scale streamwise vortex decreases with decrease of the FIH height. Moreover, 3D time-averaged large-scale arch vortical structures become stronger, the intermediate-scale arch vortices are more active.

### REFERENCES

- Rinoshika, A. and Zhou, Y., 2005, "Orthogonal wavelet multi-resolution analysis of a turbulent cylinder wake", *J. Fluid Mech.*, Vol.524, pp. 229-248.
- Rinoshika, H. and Rinoshika, A., 2019, "Passive control of a front inclined hole on flow structures around a surface-mounted short cylinder", *Ocean Eng.*, Vol.189, 106383.
- Rinoshika, H., Rinoshika, A., and Wang, J. J., 2020, "Three-dimensional multiscale flow structures behind a wall-mounted short cylinder based on tomographic particle image velocimetry and three-dimensional orthogonal wavelet transform", *Phys. Rev. E*, Vol.102, 033101.
- Sumner, D., 2013, "Flow above the free end of a surface-mounted finite-height circular cylinder: A review", *J. Fluids Struct.*, Vol.43, pp. 41-63.
- Zhu, H. Y., Wang, C. Y., Wang, H. P., and Wang, J. J., 2017, "Tomographic PIV investigation on 3D wake structures for flow over a wall-mounted short cylinder", *J. Fluid Mech.*, Vol.831, pp. 743-778.